

A classical mechanics model for the interpretation of piezoelectric property data

Andrew J. Bell

Citation: *Journal of Applied Physics* **118**, 224103 (2015); doi: 10.1063/1.4937135

View online: <http://dx.doi.org/10.1063/1.4937135>

View Table of Contents: <http://scitation.aip.org/content/aip/journal/jap/118/22?ver=pdfcov>

Published by the [AIP Publishing](#)

Articles you may be interested in

Enhanced dielectric, ferroelectric, and electrostrictive properties of $\text{Pb}(\text{Mg}_{1/3}\text{Nb}_{2/3})_{0.9}\text{Ti}_{0.1}\text{O}_3$ ceramics by ZnO modification

J. Appl. Phys. **113**, 204101 (2013); 10.1063/1.4801881

Influence of manganese doping to the full tensor properties of $0.24\text{Pb}(\text{In}_{1/2}\text{Nb}_{1/2})\text{O}_3$ - $0.47\text{Pb}(\text{Mg}_{1/3}\text{Nb}_{2/3})\text{O}_3$ - 0.29PbTiO_3 single crystals

J. Appl. Phys. **113**, 074108 (2013); 10.1063/1.4792600

Dielectric and piezoelectric activities in $(1-x)\text{Pb}(\text{Mg}_{1/3}\text{Nb}_{2/3})\text{O}_3$ - $x\text{PbTiO}_3$ single crystals from 5K to 300K

J. Appl. Phys. **111**, 104108 (2012); 10.1063/1.4716031

Grain-oriented sodium bismuth titanate-based lead-free piezoelectric ceramics prepared using the pulsed strong magnetic field and template grain growth

J. Appl. Phys. **108**, 073535 (2010); 10.1063/1.3486474

Symmetry analysis and exact model for the elastic, piezoelectric, and electronic properties of inhomogeneous and strained wurtzite quantum nanostructures

Appl. Phys. Lett. **94**, 102105 (2009); 10.1063/1.3097232



NEW Special Topic Sections

NOW ONLINE
Lithium Niobate Properties and Applications:
Reviews of Emerging Trends

AIP | Applied Physics Reviews

A classical mechanics model for the interpretation of piezoelectric property data

Andrew J. Bell^{a)}

Institute for Materials Research, School of Chemical and Process Engineering, University of Leeds, Leeds LS2 9JT, United Kingdom

(Received 2 October 2015; accepted 21 November 2015; published online 9 December 2015)

In order to provide a means of understanding, the relationship between the primary electromechanical coefficients and simple crystal chemistry parameters for piezoelectric materials, a static analysis of a 3 atom, dipolar molecule has been undertaken to derive relationships for elastic compliance s^E , dielectric permittivity ϵ^X , and piezoelectric charge coefficient d in terms of an effective ionic charge and two inter-atomic force constants. The relationships demonstrate the mutual interdependence of the three coefficients, in keeping with experimental evidence from a large dataset of commercial piezoelectric materials. It is shown that the electromechanical coupling coefficient k is purely an expression of the asymmetry in the two force constants or bond compliances. The treatment is extended to show that the quadratic electrostriction relation between strain and polarization, in both centrosymmetric and non-centrosymmetric systems, is due to the presence of a non-zero 2nd order term in the bond compliance. Comparison with experimental data explains the counter-intuitive, positive correlation of k with s^E and ϵ^X and supports the proposition that high piezoelectric activity in single crystals is dominated by large compliance coupled with asymmetry in the sub-cell force constants. However, the analysis also shows that in polycrystalline materials, the dielectric anisotropy of the constituent crystals can be more important for attaining large charge coefficients. The model provides a completely new methodology for the interpretation of piezoelectric and electrostrictive property data and suggests methods for rapid screening for high activity in candidate piezoelectric materials, both experimentally and by novel interrogation of *ab initio* calculations. © 2015 Author(s). All article content, except where otherwise noted, is licensed under a Creative Commons Attribution (CC BY) license (<http://creativecommons.org/licenses/by-cn-nd/4.0/>).

[<http://dx.doi.org/10.1063/1.4937135>]

I. INTRODUCTION

Piezoelectric materials are used extensively in modern electrotechnology, in ceramic, single crystal and thin film forms, as sensors, actuators, and signal processing devices.^{1,2} Given the wide range of applications, a variety of coefficients and figures of merit are used for assessing the suitability of piezoelectric materials for specific types of device operation. Whilst the piezoelectric charge coefficient d is generally used to assess the magnitude of the actuator response of a piezoelectric material, the piezoelectric voltage coefficient g is often regarded as the more important assessment of its sensitivity as a stress sensor. For applications that employ both the direct and converse effects in the same material element (e.g., medical imaging or sonar transducers), a more relevant figure of merit is the product $d g$. The electromechanical coupling coefficient k , which has been described as “the best single measurement of the strength of the piezoelectric effect,”³ controls the bandwidth of such transducers, directly influencing crucial performance parameters such as spatial resolution. Moreover, the permittivity ϵ is dominant in determining the electrical impedance of a piezoelectric device, the matching of which to the driving and sensing circuits is an important aspect of piezoelectric system design.

Similarly, the compliance s dominates the acoustic impedance and its match to that of the environment in which the piezoelectric device operates. Each of the three primary coefficients, s , ϵ , and d , can be considered as complex, with a relevant loss factor, $\tan \delta_i$, ($i = s, \epsilon, \text{ or } d$) being defined by the ratio of the imaginary to real parts. Whilst losses are an important issue in materials selection for piezoelectric applications, they are not the primary concern of this paper, which addresses only the real components.

Optimization of the above set of coefficients for specific applications is the primary goal of materials engineers developing new or existing piezoelectric materials. Whilst much effort has been expended on understanding the extrinsic (domain) contributions to materials such as $\text{Pb}(\text{Zr}, \text{Ti})\text{O}_3$,⁴ the non-empirical optimization of the intrinsic properties in terms of the three material coefficients and k requires a degree of insight into the influence of crystal parameters on the mechanisms of piezoelectricity that has not yet been achieved. This is compounded by the fact that the three primary coefficients, d , s , and ϵ , are not independent variables, as will be demonstrated below. Despite well established relationships to calculate k from the measured properties s , ϵ , and d , it is not immediately obvious how the compliance and polarizability of a given structure couple at the unit cell level to maximize energy conversion in terms of ion displacements. Whilst *ab initio* calculations can provide some

^{a)}E-mail: a.j.bell@leeds.ac.uk



guidance to the materials engineer, they do not provide the type of simple, intuitive insights of how the primary coefficients are inter-related via crystal chemical parameters that can be valuable in guiding experimental materials discovery. This paper therefore explores a simple classical mechanics approach to describe the mechanism of piezoelectricity in the simplest of structures and thereby elucidates the relationships between the primary coefficients and the coupling coefficient.

First, the paper establishes the premise that the three primary coefficients s , ϵ , and d are not independent, by correlating data from a large set of commercial piezoelectric materials. Second, it examines the applicability of simple discrete, dipolar structures as surrogates for extended piezoelectric crystals, and selects a three-atom, asymmetric molecule as the preferred model. Third, it derives expressions for the primary coefficients, in terms of ionic charges, molecular dimensions, and inter-atomic bond strengths, expressed as Hookian spring constants. By considering a symmetric version of the model, it also shows how that the existence of electrostriction requires the inter-atomic bonds to have a non-linear compliance. To test the effectiveness of the model, the model parameters are calculated from the measured property coefficients for each of the members of the aforementioned dataset. Conclusions are drawn concerning the mutual independence and relative importance of the effective dipolar charge and bond strength asymmetry in determining intrinsic piezoelectric properties of real materials. How the model applies to a number classical examples of piezoelectric materials is examined in detail, providing additional insight into a number of phenomena, including the differences between single crystals and ceramics.

II. DEFINITIONS

The most fundamental form of electromechanical coupling in all solids is known as electrostriction⁵ and for centrosymmetric structures is represented as the relationship between the induced strain, x , and the even powers of the electric field, E

$$x = m_1 E^2 + m_2 E^4 + \dots \quad (1)$$

For weak fields, it is normal for the first term to dominate, but the higher order terms are often significant at fields below the breakdown field in a manner similar to the non-linearity between field and polarization. Hence, in practice it is often found that the parametric relationship between induced strain and polarization P is better behaved, as the non-linearities in permittivity are eliminated and higher order terms suppressed

$$x = QP^2. \quad (2)$$

Q is referred to hereafter as the electrostriction coefficient. Despite the simplicity of the relationship, there is no simple, intuitive model which allows derivation of this coefficient from other material parameters.⁶⁻⁸

In most non-centrosymmetric solids, the phenomenon of piezoelectricity⁹ is the dominant form of electromechanical

coupling and under weak fields the intrinsic effect is regarded as a linear phenomenon. The change of polarization as a function of stress is known as the direct piezoelectric effect, whilst a change in strain as a function of electric field is known as the converse effect. They are described by the constitutive relationships that relate changes in strain x and dielectric displacement D to the application of stress X and electric field E

$$x = s^E X + dE, \quad (3)$$

$$D = dX + \epsilon^X E. \quad (4)$$

These equations define the three material coefficients essential for describing electromechanical behaviour: the elastic compliance at constant field s^E , the piezoelectric charge coefficient d , and the dielectric permittivity at constant stress ϵ^X , which are referred to herein as the *primary* coefficients. The electromechanical coupling coefficient is defined as the square root of the fraction of energy converted from mechanical to electrical energy (or vice versa) with respect to the input energy

$$k^2 = \frac{\text{converted energy}}{\text{input energy}}. \quad (5)$$

It can be shown that k is related to the three primary material coefficients by³

$$k^2 = \frac{d^2}{s^E \epsilon^X}, \quad (6)$$

which is the most widely used of the equivalent expressions in the determination of k .

III. INTERDEPENDENCE OF THE PRIMARY COEFFICIENTS

Data for d , s^E , and ϵ^X , along with the electromechanical coupling coefficient k , have been collected for 116 piezoelectric materials from the on-line data sheets of 13 well-established manufacturers of piezoelectric materials.¹⁰ The set includes data for “hard” and “soft” $\text{Pb}(\text{Zr}, \text{Ti})\text{O}_3$ ceramics ($0.6 < k_{33} < 0.8$), for lead-free piezoelectric ceramics ($k_{33} < 0.6$) and perovskite single crystals ($k_{33} > 0.8$), with a range of d_{33} values covering more than two orders of magnitude. The use of a large set of commercial data is justified over a necessarily smaller set of scientific literature values, as the data are corroborated and subjected to scrutiny on an almost daily basis by the manufacturers and, more critically, by their customers. In addition, the scientific literature contains relatively, few examples, of self-consistent data in which d , s^E , and ϵ^X are all provided.

Figure 1 shows plots of k_{33} against (a) d_{33} , (b) s_{33}^E , and (c) ϵ_{33}^X for the large dataset. In part agreement with Eq. (6), k_{33} increases as a function of increasing d_{33} , but not in a linear manner. For the larger values of d_{33} , k_{33} appears to increase asymptotically towards unity. It might be expected from Eq. (6) that the coupling coefficient would be inversely correlated with both s_{33}^E and ϵ_{33}^X . However, as shown in Figs. 1(b) and 1(c), the dependence of k_{33} upon both s_{33}^E and ϵ_{33}^X is

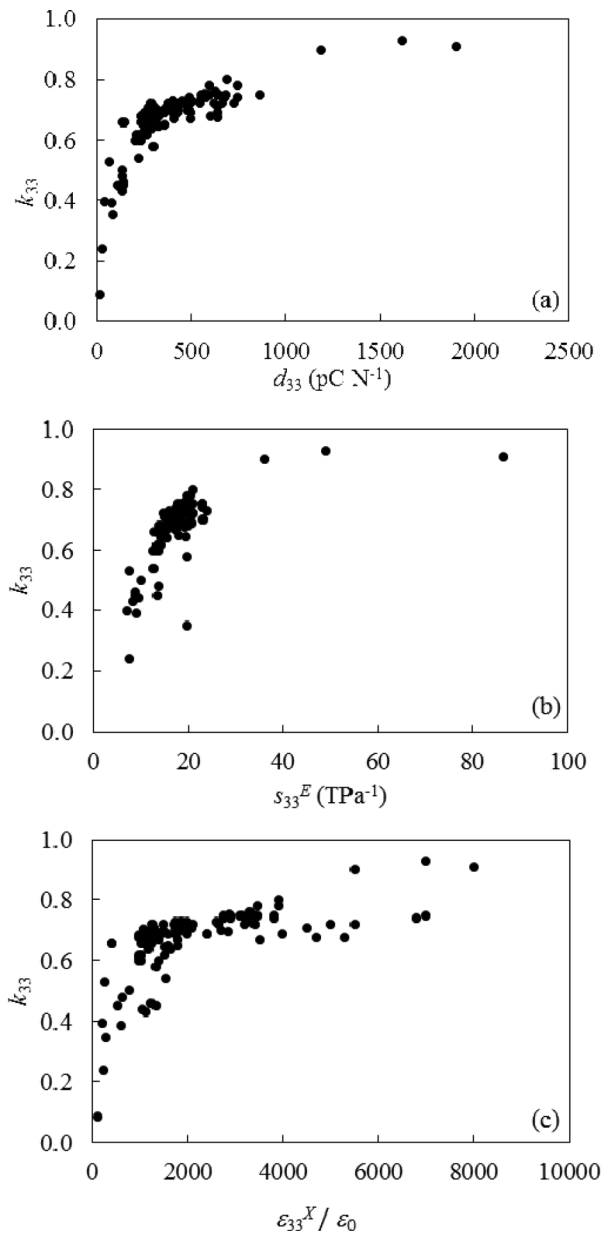


FIG. 1. (a) k_{33} vs d_{33} (b) k_{33} vs s_{33}^E and (c) k_{33} vs ϵ_{33}^X for a set of 116 piezoelectric materials, encompassing PZT, lead free ceramics, and $\text{Pb}(\text{Mg}_{1/3}\text{Nb}_{2/3})\text{O}_3$ -based single crystals.

contrary to that expectation. Indeed, increasing either s_{33}^E or ϵ_{33}^X appears to result in k_{33} increasing in a similar manner to its dependence on d_{33} .

Figure 2 shows a plot of ϵ_{33}^X vs. d_{33} for the same dataset, establishing that there is clear interdependence between the two. Depending on whether the three outlying, single crystal data points with large ϵ_{33}^X and d_{33} are included, the correlation might be interpreted as linear or quadratic. The data demonstrate why piezoelectric materials optimization can be challenging; from Eq. (6) maximization of k would normally be expected by minimizing s_{33}^E and ϵ_{33}^X , but the data show that the opposite trend is more realistic. This interdependence of the three primary coefficients inhibits an intuitive approach to piezoelectric materials engineering and has motivated the derivation of the following simple model to clarify the form of the interdependence of the coefficients.

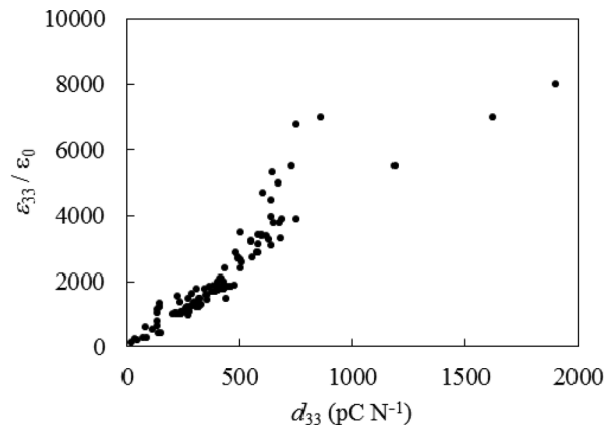


FIG. 2. ϵ_{33}^X vs d_{33} for the dataset of Figure 1.

IV. THEORETICAL

A. A surrogate model for a piezoelectric crystal

To better understand the relationships between the four coefficients, d , s^E , ϵ^X , and k , it is proposed to undertake a static, classical mechanics analysis of a simple arrangement of ions, which represents the key elements of a piezoelectric material, i.e., a lack of centre of symmetry and, to cater for the case of ferroelectric materials, the capacity for a permanent dipole moment. A preferred model would be an infinite, one-dimensional, diatomic chain (Fig. 3(a)); however, definitive analysis of extended polar structures is non-trivial due to the known problem of polarization ambiguity.¹¹ Hence, as surrogate models for the origin of crystal piezoelectric properties, two different dipolar units are considered: (i) a simple two atom dipole and (ii) a three atom, asymmetric ‘‘molecule.’’

One might consider a simple dipole as in Fig. 3(b) comprising two point charges and a single bond as a surrogate for the chain; however, whilst the unit is itself asymmetric, a simple translational array of this unit (e.g., the NaCl structure) would be centrosymmetric. Also an analysis of a simple dipole employing Eqs. (3), (4), and (6) yields the unrealistic result $k = 1$.

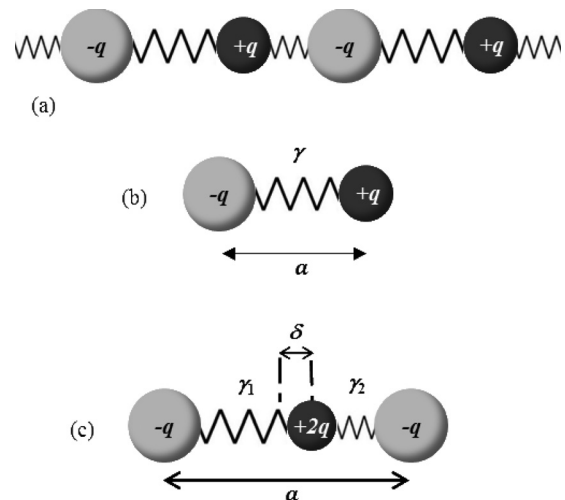


FIG. 3. (a) Diatomic chain model and (b) simple dipole and (c) three atom dipolar molecule.

A more appropriate model is of a non-centrosymmetric molecule comprising an ion with positive charge $+2q$ displaced by distance δ from the central position between two ions with charges $-q$ (Fig. 3(c)), with the distance between the two negative ions being a and a molecular volume v . The two interatomic bonds are characterised by the two inverse force constants γ_1 and γ_2 , generally defined by the change in length of the bond Δa on application of a force, F

$$\Delta a = \gamma F. \quad (7)$$

A similar schematic concept was introduced by Murlant in Ref. 12, but without the following mathematical treatment.

As the molecule is charge neutral, its spontaneous polarization can be defined unambiguously as a function of δ as

$$P_s = 2q\delta/v. \quad (8)$$

The primary coefficients are again derived by applying Eqs. (3) and (4) to determine the strain and change in polarization as a function of field and stress

$$s^E = \frac{v}{a^2}(\gamma_1 + \gamma_2), \quad (9)$$

$$\varepsilon^X \approx \varepsilon_0 \chi^X = \frac{q^2}{v}(\gamma_1 + \gamma_2), \quad (10)$$

and

$$d = \frac{q}{a}(\gamma_1 - \gamma_2). \quad (11)$$

The expression for d is independent of whether it is derived from Eq. (3) or (4). Note that the susceptibility χ^X is considered equal to the relative permittivity $\varepsilon^X/\varepsilon_0$ for cases where $\varepsilon^X > 10\varepsilon_0$; this approximation is applied consistently here, unless stated otherwise

Combining the three coefficients according to Eq. (6) gives an expression for the coupling coefficient

$$k = \frac{\gamma_1 - \gamma_2}{\gamma_1 + \gamma_2}. \quad (12)$$

Unsurprisingly, s^E is only dependent upon the sum of the bond compliances and geometric factors. The permittivity is dependent upon the sum of the bond compliances and the square of the effective charge, whereas the charge coefficient d is linearly dependent upon the effective charge, and, crucially, the difference between the two compliances. Perhaps most interestingly, the coupling coefficient is dependent only on the two force constants and can be interpreted as an expression of the asymmetry in the interatomic bonding. This suggests that the coupling coefficient, which is quite often regarded as simply a device figure of merit, is actually a rather fundamental materials concept, expressing the relative importance of the asymmetry in interatomic bonding. For $\gamma_1 = \gamma_2$, implying a centrosymmetric structure, $k = 0$, whereas for maximum asymmetry ($\gamma_1 \gg \gamma_2$), the model tends towards that for the simple dipole with $k \approx 1$. It should be noted that the expressions (9)–(12) are valid when $\delta = 0$. A spontaneous polarization is not required to sustain

piezoelectricity; asymmetry in the bonds is the minimum requirement.

Standard alternative expressions of the coupling coefficient to that in Eq. (6) are in terms of the ‘‘clamped coefficients’’:³ the permittivity at constant strain ε^x and the compliance at constant displacement s^D , where

$$k^2 = 1 - \frac{\varepsilon^x}{\varepsilon^E} = 1 - \frac{s^D}{s^E}. \quad (13)$$

The derivation of the clamped coefficients for the 3 atom molecule provides a test of the self-consistency of the model. The derivation of ε^x is undertaken independent of Eq. (10), by applying both field and stress simultaneously according to Eq. (4), so that strain is maintained at zero, giving

$$\varepsilon^x = 4 \frac{q^2}{v} \frac{\gamma_1 \gamma_2}{\gamma_1 + \gamma_2}. \quad (14)$$

A similar approach for the compliance reveals

$$s^D = 4 \frac{v}{a^2} \frac{\gamma_1 \gamma_2}{\gamma_1 + \gamma_2}. \quad (15)$$

Eq. (13) therefore becomes $k^2 = 1 - 4 \frac{\gamma_1 \gamma_2}{(\gamma_1 + \gamma_2)^2}$, which is identical to the expression in (12) and confirms that Eqs. (9), (10), (14), and (15) accord with the definition of Eq. (13).

Either Eq. (3) or (4) with (9)–(11) can be used to derive an expression for the spontaneous strain of the structure, i.e., the change in a when sufficient field or stress is applied to render $\delta = 0$

$$x_s = \frac{\Delta a}{a} = \frac{2\delta \gamma_1 - \gamma_2}{a \gamma_1 + \gamma_2} = \frac{2\delta}{ak}. \quad (16)$$

This implies that the magnitude of the coupling coefficient should be evident not only from the asymmetry in the internal force constants of a structure but also for a ferroelectric, by a comparison of the geometry in the polar and non-polar phases

$$k = \frac{2\delta}{\Delta a}, \quad (17)$$

where Δa and δ are the change in polar lattice spacing and polar ion shift on passing through the ferroelectric phase transition.

B. Non-linearity and electrostriction

It is interesting to explore whether the 3 atom model is also consistent with the relationship between electrostriction and piezoelectricity defined from the derivative of Eq. (2)

$$d = \frac{dx}{dE} = 2QP \frac{dP}{dE} = 2QP\varepsilon^X. \quad (18)$$

Electrostriction is present in both centrosymmetric and non-centrosymmetric solids; in the first instance, the centrosymmetric case is considered. Taking the 3 atom model, but with $\delta = 0$ and $\gamma_1 = \gamma_2 = \gamma$, it is trivial to show that on applying an electric field, E , one bond will contract by γEq whilst the

other extends by the same distance, hence, despite a resultant polarization of $2\gamma E q^2/\nu$, there is no overall change in length of the molecule. In this case, the electrostriction coefficient would be zero. However, if the bond compliance is non-linear such that

$$\Delta a = \gamma F + \eta F^2, \quad (19)$$

on application of an electric field, the two bonds will change their lengths by

$$\delta_1 = \gamma E q + \eta E^2 q^2 \quad \text{and} \quad \delta_2 = -\gamma E q + \eta E^2 q^2, \quad (20)$$

respectively. Hence the change in length of the molecule is

$$\delta_1 + \delta_2 = 2\eta E^2 q^2, \quad (21)$$

equivalent to a strain of

$$x = \frac{2\eta E^2 q^2}{a}. \quad (22)$$

The displacement of the central ion δ is

$$\delta = \frac{\delta_1 - \delta_2}{2} = \gamma E q, \quad (23)$$

giving a polarization of

$$P = \frac{2\gamma E q^2}{\nu}, \quad (24)$$

identical to that in the linear elastic case.

Thus, the electrostriction coefficient is given by

$$Q = \frac{x}{P^2} = \frac{1}{2} \frac{\nu^2}{a} \frac{\eta}{\gamma^2 q^2}, \quad (25)$$

and is directly proportional to the second order bond compliance, η . Also notable is the reciprocal dependence of Q on q^2 ; as permittivity is directly proportional to q^2 , the relationship in Eq. (25) is consistent with the empirical observation of a correlation between permittivity and $1/Q$ for a wide range of materials.¹³ Electrostriction only exists if the compliance of the molecule is non-linear; the treatment allows for higher order terms in the compliance; however, only the even order terms would appear in the electrostriction relation.

C. Elastic non-linearity and piezoelectricity

How does the inclusion of elastic non-linearity modify the identities for piezoelectric coefficients? This is explored through the assumption of an internal bias field E_i applied to the symmetric case in order to provide bond asymmetry and produce a spontaneous polarization

$$P_s = \frac{2\gamma q^2}{\nu} E_i. \quad (26)$$

Applying Eqs. (3) and (4) gives

$$s^E = \frac{2\gamma\nu}{a^2} + \frac{2\eta\nu^2}{a^3} X, \quad (27)$$

$$\epsilon^X = \frac{2\gamma q^2}{\nu}, \quad (28)$$

$$d = \frac{4\eta q^2 E_i}{a} + \frac{4\eta q^2}{a} E. \quad (29)$$

The elastic non-linearity is, of course, self-evident in the expression for compliance, but, as in the centrosymmetric case, has no influence on the permittivity. For the charge coefficient, the additional applied-field dependent term is only apparent in the converse d coefficient ($= dx/dE$) as shown in Eq. (29), whilst the direct coefficient ($= dP/dX$) remains linear.

Under the weak field assumption, in which the linear contributions to s^E and d dominate, the coupling coefficient is

$$k = \frac{2\eta E_i q}{\gamma}. \quad (30)$$

In this context, the coupling coefficient appears to be a consequence of the elastic nonlinearity, η/γ with the asymmetry provided by the internal field, E_i .

In the non-linear model, at non-zero internal bias, the two bonds have different values of compliance with respect to field or stress modulation. Hence, in the weak, applied field limit, the model is actually identical to the original ‘‘linear’’ model, which assumed different bond compliances as the starting point. The linear model bond compliances in terms of the non-linear parameters are

$$\gamma_1 = \gamma + 2\eta q E_i \quad (31)$$

and

$$\gamma_2 = \gamma - 2\eta q E_i. \quad (32)$$

V. COMPARISON OF THE MODEL WITH EXPERIMENTAL DATA

This section addresses whether the above three atom model is relevant to the complexity embodied in real materials and reveals the relative importance of the model parameters (q , γ_1 and γ_2 or q , γ , η , and E_i) in determining the properties of common piezoelectric materials. Hence, in the following, the 3 atom model parameters are determined for a range of real materials. It should be noted that the parameterization treats the piezoelectric measurement data as if they were obtained from a black-box; i.e., the model is ignorant of form (single crystal or polycrystal), crystal symmetry or direction of measurement with respect to the polar axis.

A. Electrostriction

First, the case of electrostriction in centrosymmetric materials is considered. As most crystals do not exhibit significant non-linearity in their elastic properties, it is pertinent to explore the importance of the non-linear elastic term implied by the electrostriction coefficient in a real case. Considering a simple cubic crystal, such as NaCl, at low stress the linear term in the compliance may be considered dominant, hence we can estimate γ as equal to $s^E/2a$.

The coefficient η can then be estimated from Eq. (25) rewritten as

$$\eta = \frac{s^E \varepsilon_0 \chi^X Q}{2a^3}. \quad (33)$$

In this case, due to the low permittivity of NaCl ($\varepsilon^X = 6\varepsilon_0$), the expression is given in its precise form in terms of susceptibility χ^X . From Ref. 6, the value of Q_{1111} for NaCl is determined as $1.7 \text{ m}^4 \text{ C}^{-2}$, with s_{11}^E given as $22.9 \times 10^{-12} \text{ m}^2 \text{ N}^{-1}$. With $a = 5.64 \text{ \AA}$ and $\chi^X = 5$, a value for η of $4.80 \times 10^6 \text{ m N}^{-2}$ is calculated. This second order coefficient appears considerably larger than the linear coefficient $\gamma \approx 0.02 \text{ m N}^{-1}$. However, given that for a stress of 10 MPa, an equivalent force on a single NaCl unit cell is approximately 3 pN, the linear term in Eq. (19) dominates until applied stresses well beyond 10 GPa. Hence, the model suggests that although a material may appear to be a linear elastic, a relatively small elastic non-linearity can be revealed through a finite electrostrictive coefficient, even under weak electric fields, due to cancellation of the linear components of compliance in a dipolar structure.

B. The relationship between k and s^E , ε^X , and d

The model allows a better understanding of the relationship illustrated in Fig. 1 between the primary coefficients and k . Eliminating γ_2 and γ_1 in turn from the expressions in Eqs. (9)–(11) reveals two simple relationships between d , ε^X , and s^E

$$d = d_1 - \sqrt{s^E \varepsilon^X}, \quad d = \sqrt{s^E \varepsilon^X} - d_2, \quad (34)$$

where

$$d_1 = \frac{2q\gamma_1}{a} \quad \text{and} \quad d_2 = \frac{2q\gamma_2}{a} \quad (35)$$

equivalent to twice the piezoelectric charge coefficients of simple dipoles, with reciprocal force constants γ_1 and γ_2 , respectively. From Eqs. (6) and (34), the relationship between d and k can be expressed as

$$k = \frac{d}{d_1 - d} = \frac{d}{d_2 + d}. \quad (36)$$

Figure 4 plots the function $k = \frac{d}{d_2 + d}$ for values of $d_2 = 50, 150,$ and 300 pC N^{-1} , together with the data from Fig. 1(a) for the large commercial dataset. It can be seen that the function is a good representation of the correlations between the material data. All the data fall between the lines for $d_2 = 50$ and 300 pC N^{-1} , with the majority of the data clustered around the line for $d_2 = 150 \text{ pC N}^{-1}$. An understanding of the meaning of d_2 from Eq. (34) is that it is the difference between the actual value of the d coefficient and its potential maximum at $k=1$ represented by $\sqrt{s^E \varepsilon^X}$. Similar relationships between s^E and k and between ε^X and k can be derived from Eqs. (9)–(12) which also explain the form of the correlations in Figs. 1(b) and 1(c)

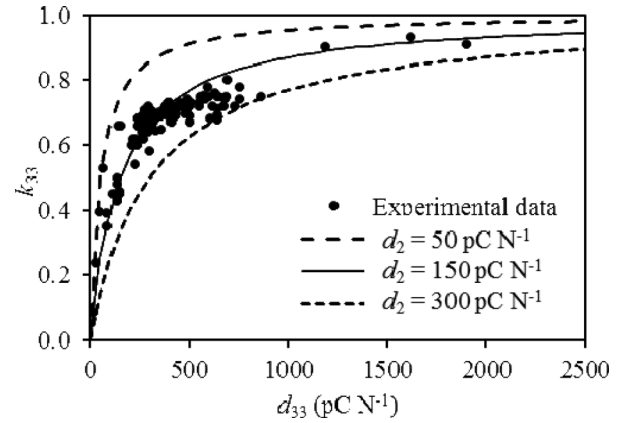


FIG. 4. k as a function of d ; data-points are for the data set of Fig. 1(a); the lines illustrate the relationship $k = d/(d + d_2)$ for values of $d_2 = 50, 150,$ and 300 pC N^{-1} .

$$k = \frac{s^E - s_1}{s^E} = \frac{s_2 - s^E}{s^E}, \quad \text{with} \\ s_1 = \frac{2v\gamma_1}{a^2} \quad \text{and} \quad s_2 = \frac{2v\gamma_2}{a^2} \quad (37)$$

and

$$k = \frac{\varepsilon^X - \varepsilon_1}{\varepsilon^X} = \frac{\varepsilon_2 - \varepsilon^X}{\varepsilon^X}, \quad \text{with} \\ \varepsilon_1 = \frac{2q^2\gamma_1}{v} \quad \text{and} \quad \varepsilon_2 = \frac{2q^2\gamma_2}{v}. \quad (38)$$

Hence, the 3 atom treatment has yielded a set of equations which explicitly demonstrate the interrelationships between k and d , ε^X and s^E . The form of the relationships matches that of the correlations between the coefficients exhibited by a large dataset of commercial piezoelectric materials.

C. Commercial piezoelectric materials dataset

To determine the relative importance of the model parameters to a range of piezoelectric materials, the large dataset of Figs. 1 and 2 is analysed. Due to the absence of P_s values from the set, the “linear” model parameters will be employed. The values of the q , γ_1 , and γ_2 are calculated from the data for d_{33} , s_{33}^E , and ε_{33}^X using Eqs. (9)–(11). The molecule length and molecular volume and are equated to the lattice parameter and unit cell volume, respectively. As these are not known precisely for each member of the set, the unit cell parameters and volumes will be assumed constant for the whole set as virtually all the materials are perovskites with lattice parameters of approximately 4 \AA . For example, at room temperature, the parameters of tetragonal barium titanate are $a = 3.992 \text{ \AA}$ and $c = 4.036 \text{ \AA}$, for tetragonal lead titanate $a = 3.901 \text{ \AA}$ and $c = 4.149 \text{ \AA}$, and for rhombohedral PMN-PT $a = 4.014 \text{ \AA}$. Hence, for the following analysis, it is assumed that all the materials in the dataset have a lattice parameter of 4.0 \AA and correspondingly have a unit cell volume, $v \approx a^3 = 64 \times 10^{-30} \text{ m}^3$. It is recognized that this

TABLE I. Average values and ranges of s_{33}^E , ϵ_{33}^X , d_{33} , and k_{33} for the dataset together with the same details of the calculated values of q , γ_1 , and γ_2 .

Parameter	Average	Minimum	Maximum	Units
s_{33}^E	18.2	7.31	86.5	TPa ⁻¹
ϵ_{33}^X	2134	124	7996	nF m ⁻¹
d_{33}	410	19.1	1900	pC N ⁻¹
k_{33}	0.67	0.09	0.93	
q	30.77	4.98	58.66	e ($=1.6 \times 10^{-19}$ C)
γ_1	37	1.2	191	Mm N ⁻¹
γ_2	6.5	1.6	25.1	Mm N ⁻¹

assumption represents a source of scatter in some of the data correlations below.

From Eqs. (9) and (11), the effective dipolar charge for each material can be calculated from

$$q = \frac{v}{a} \sqrt{\frac{\epsilon_{33}^X}{s_{33}^E}}, \quad (39)$$

whilst

$$\gamma_1 = \frac{1}{2} \left(\frac{a^2}{v} s_{33}^E + \frac{a}{q} d_{33} \right) \quad (40)$$

and

$$\gamma_2 = \frac{1}{2} \left(\frac{a^2}{v} s_{33}^E - \frac{a}{q} d_{33} \right). \quad (41)$$

Note that the subscript ‘‘33’’ denotes a measured value from the dataset, as distinct from the model results in Eqs. (9)–(11).

In effect, Eqs. (39)–(41) parameterize the s_{33}^E , ϵ_{33}^X , and d_{33} data in terms of an effective dipolar charge and the two bond compliances. The average values and ranges of s_{33}^E , ϵ_{33}^X , d_{33} , and k_{33} for the dataset together with the same details of the calculated values of q , γ_1 , and γ_2 are shown in Table I. Plots of each of the primary coefficients against each of the parameters are shown in Fig. 5. In order to emphasize the trends for the majority of the samples, the data for the three PMN-PT crystals have been omitted from Fig. 5 and will be discussed separately below. A number of relationships become apparent in Fig. 5. Whilst s_{33}^E has no apparent correlation with the value of q , both ϵ_{33}^X and d_{33} are strongly correlated with q . Due to the lack of data at very low ϵ_{33}^X , it is not possible to say, whether the form of the correlation is quadratic or linear for ϵ_{33}^X . Unsurprisingly, as $\gamma_1 \gg \gamma_2$ for the majority of materials in the dataset, s_{33}^E correlates linearly with γ_1 . The correlations of ϵ_{33}^X and d_{33} with γ_1 are less strong, but clearly both increase with increasing γ_1 . There is no obvious dependence of any of the coefficients on γ_2 . However, γ_2 certainly plays role in determining k_{33} , as a plot of k_{33} vs γ_1 is well correlated, although not linearly (Fig. 6(a)), whilst k_{33}

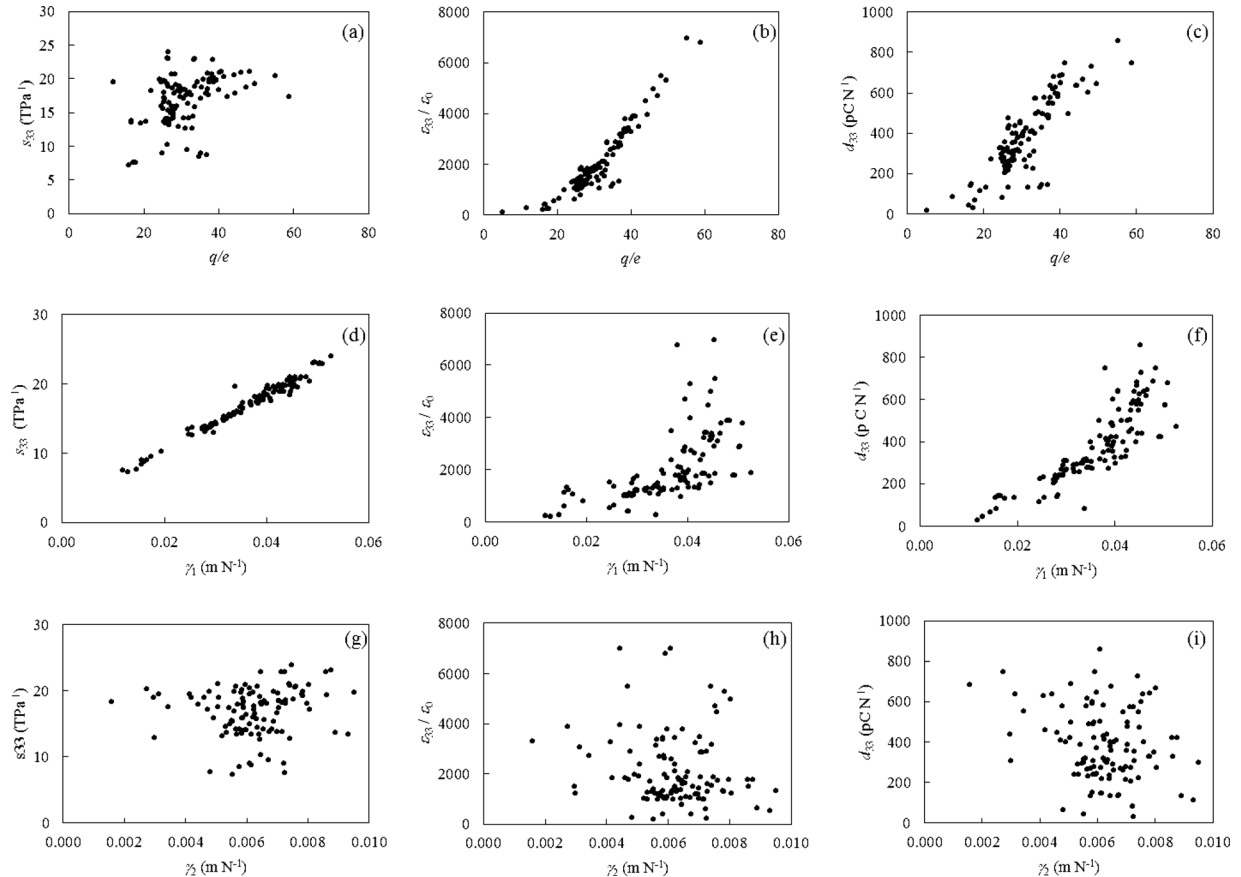


FIG. 5. The primary coefficients s_{33}^E , ϵ_{33}^X , and d_{33} plotted against the model parameters, q , γ_1 and γ_2 , for the large commercial dataset. For clarity, the outlying datapoints for PMN-PT single crystals are omitted.

vs $(\gamma_1 - \gamma_2)/(\gamma_1 + \gamma_2)$ shows a strong linear relationship (Fig. 6(b)), the scatter of which is due to the experimental values of k_{33} not being consistent with those for s_{33}^E , ϵ_{33}^X , and d_{33} for some members of the dataset.

In general, the analysis shows that there is good consistency in the generation of the model parameters from experimental data and that whilst q and γ_1 are the two most important parameters, both γ_1 and γ_2 are required to accurately reproduce k .

Given that a motivation for the model was to account for the interdependence of the 3 primary coefficients, it is important that the model parameters are actually mutually independent. Figure 7 shows plots of (a) γ_1 vs γ_2 , (b) q vs γ_1 , and (c) q vs γ_2 for the dataset. There are no discernible correlations in any of the plots, indicating that the three parameters are indeed mutually independent.

D. Comparative examples

As the large commercial dataset mainly comprises data from incompletely specified ceramics, without precise lattice parameters or values of spontaneous polarization, a more critical analysis of the utility of the parameterization requires a set of more rigorously self-consistent data. Table II shows literature values of the electromechanical coefficients for a number of representative piezoelectrics, together with values for the crystal dimension along the measurement axis (a) and the unit cell volume (v). The calculated model parameters

are presented for the linear and also, in the case of ferroelectrics, for the non-linear treatments. The materials set includes examples of the non-ferroelectric piezoelectrics AlN and ZnO,¹⁴ plus the classic ferroelectric crystals BaTiO₃,³ KNbO₃,¹⁵ and PbTiO₃.³ For comparison, data from polycrystalline materials^{3,10} and from Landau-Ginzburg-Devonshire (LGD) calculations^{16,17} are included for BaTiO₃ and PbTiO₃. In the case of PZT, ceramic data for hard and soft commercial materials¹⁰ are tabulated, however despite the availability of LGD calculations for PbZr_{0.5}Ti_{0.5}O₃ single crystals,¹⁸ analysis has not been possible due to the lack of reliable compliance or coupling coefficient data. Measured data for PMN-PT is given for samples poled parallel to the [100] and [111] directions and measured parallel to the poling direction.¹⁹

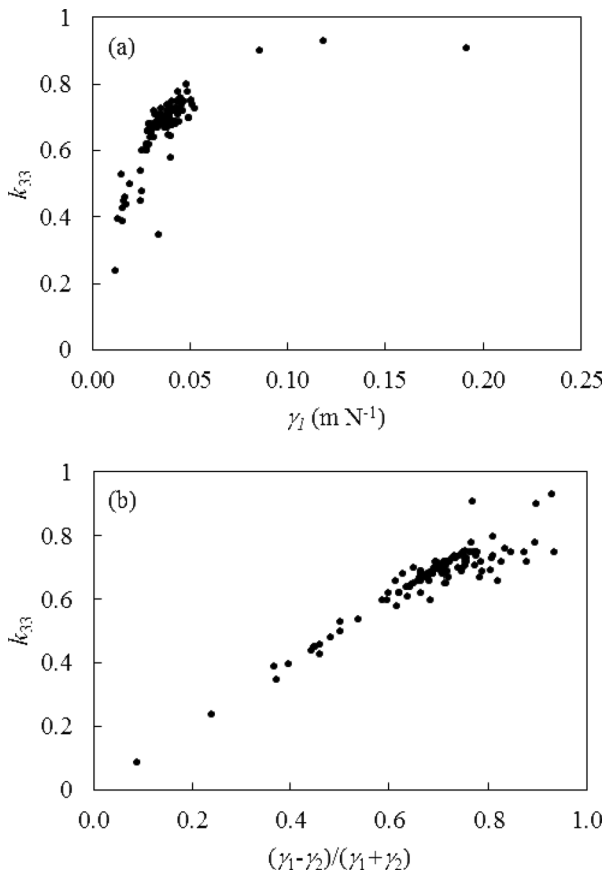


FIG. 6. (a) k_{33} vs γ_1 and (b) k_{33} vs. $(\gamma_1 - \gamma_2)/(\gamma_1 + \gamma_2)$ for the complete data set (including PMN-PT crystals).

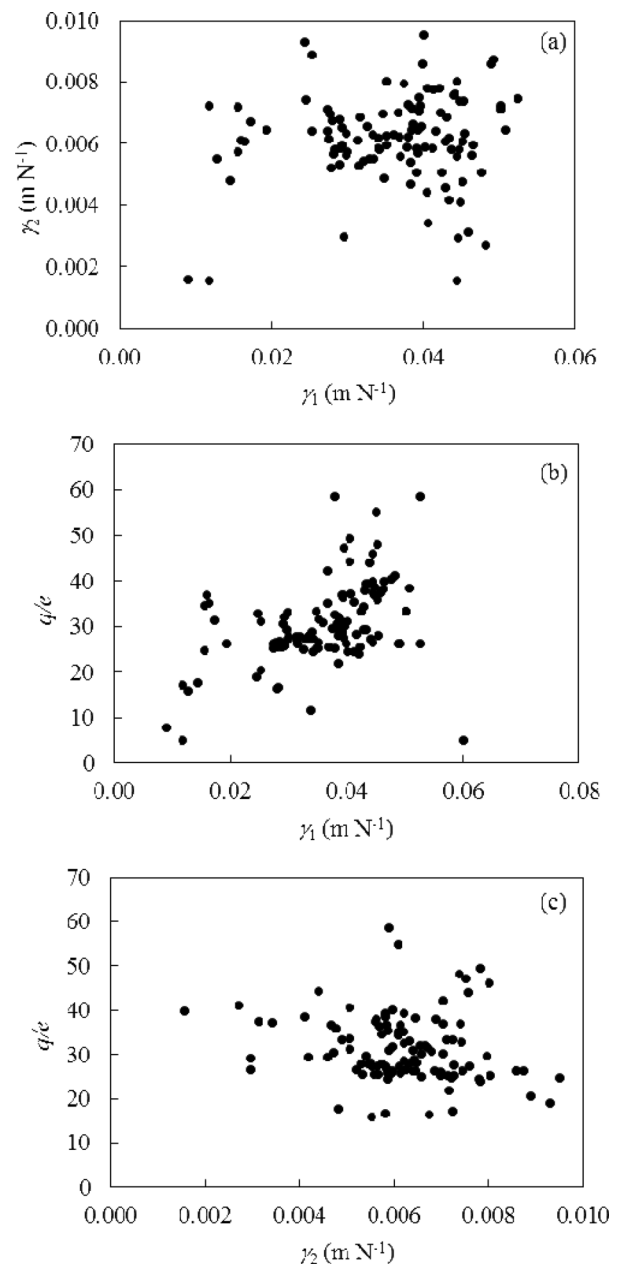


FIG. 7. (a) γ_1 vs γ_2 , (b) q vs γ_1 , and (c) q vs γ_2 for the dataset.

It is readily observed that the non-ferroelectric piezoelectrics owe their inferior d coefficients to a combination of low effective charge, q , high stiffness (low γ_1), and a small ratio of γ_1 to γ_2 when compared to the ferroelectric examples. Although KNbO_3 has a similar compliance to ZnO , both q and γ_1 of KNbO_3 are twice those of ZnO , with a significantly larger γ_1/γ_2 ratio, accounting for the larger d value (Fig. 8).

In a similar vein, γ_1 and q of BaTiO_3 are both larger than those of KNbO_3 resulting in a significantly larger permittivity and charge coefficient, despite the larger spontaneous polarization of KNbO_3 , which is a consequence of the large effective internal field value (E_i). It is reassuring that the analysis provides similar results for the experimental and LGD model data for single crystal BaTiO_3 .

The data for crystal PbTiO_3 , taken from the thermodynamic model of Haun,¹⁷ show that despite a relatively large value of γ_1 , consistent with the large compliance value, the charge coefficient is rather low, due to the low value of effective charge, q . As in KNbO_3 , the large spontaneous polarization is due to the large internal field, rather than a large effective charge. Indeed, there is a clear trend in the data of Table II suggesting that E_i is inversely proportional to q , indicating that the non-linear parameters may not be as mutually independent as the linear parameters.

For ceramic BaTiO_3 and PbTiO_3 , the calculated effective charges are significantly larger and the bond compliances lower than in the equivalent single crystals. It is noted that the parameters for PZT ceramics may also follow this trend. This apparent discrepancy can be understood as follows. In polycrystalline materials, the properties are derived from an averaging of the angular variation in properties of the equivalent single crystal. For example, in single crystal BaTiO_3 , at room temperature, the values of relative permittivity and compliance, parallel and perpendicular to the [001] polar axis are $\epsilon_{33}^x/\epsilon_0 = 168$, $\epsilon_{11}^x/\epsilon_0 = 2920$, $s_{33}^E = 15.7 \text{ TPa}^{-1}$, and $s_{11}^E = 8.93 \text{ TPa}^{-1}$.⁶ Whilst the ‘‘dielectric compliance’’ is almost 20 times greater perpendicular to the polar axis, the elastic compliance is almost half of the polar axis

value. Hence, a polycrystalline material will appear to be elastically stiffer, but with a larger permittivity than the single crystal counterpart. When subject to the analysis presented above, the effective charge of the ceramic is larger and bond compliance lower than for the single crystal. Extrapolating to the general case, whilst compliance asymmetry parallel to the polar axis is the dominant characteristic in determining single crystal piezoelectric performance, in ceramics the dielectric anisotropy of the crystal plays a much greater role. The model is thus consistent with other approaches to understanding the origins of high piezoelectric response in ceramics, particularly close to instabilities.²⁰

The single crystal data for BaTiO_3 implies from Eqs. (9) and (10) that $q/e = 54.23$ and $\gamma_1 = \gamma_2 = 11 \text{ mm N}^{-1}$ along [100] compared to $q/e = 9.7$ and $\gamma_1 = 30.98$ and $\gamma_2 = 8.75 \text{ mm N}^{-1}$ along the polar [001] axis. The effective charge perpendicular to the polar axis appears to be 5 times greater than that parallel to it. This result is not so intuitive in terms of the classical mechanics approach, in which the charges are considered to be fixed in value, but the crystal structure is flexible. The significance of such large anisotropy in the effective charge has yet to be fully understood, but in real crystals, as the effective charge q is probably related to a mean of the ionic charges weighted according to their displacements, the charge anisotropy may be due to the variation in the number and type of ions which can effectively contribute to the induced polarization as a function of the direction of the applied field.

A further source of variance between single crystal and ceramic data is that ceramics are more liable to be influenced by the presence of 180° domain walls. The majority of materials in the large commercial dataset are PZT, covering a large range of d_{33} values from 250 to 700 pC N^{-1} , for which domain wall contributions are the most likely source of variation. It can be assumed that domain walls are also the origin of the differences in the properties of the hard and soft PZT ceramics in Table III, resulting in almost a factor of 2 difference in both permittivity and charge coefficient. Whilst the

TABLE II. Experimental or theoretical values of electromechanical properties of selected piezoelectric materials with the resulting calculated model parameters; the cited references are for the origin of the property values.

Material	Measured properties						Linear parameters				Non-linear parameters				Reference
	a \AA	v \AA^3	s_{33}^E TPa^{-1}	$\epsilon_{33}^x/\epsilon_0$	d_{33} pC N^{-1}	k_{33}	P_s C m^{-2}	γ_1 mm N^{-1}	γ_2 mm N^{-1}	q/e	E_i MV m^{-1}	γ mm N^{-1}	η Mm N^{-2}	δ pm	
AlN	4.98	47.9	2.64	11.9	5	0.3	...	8.88	4.78	3.8	14
ZnO	5.21	55.2	6.99	11.26	12	0.47	...	25.23	9.19	2.5	14
KNbO_3 crystal	5.36	66.00	6.44	44	30	0.59	0.30	22.17	5.70	6.0	777.1	14.02	11.2	10.38	15
BaTiO_3 crystal (LGD)	4.036	64.38	13.10	188	95	0.64	0.26	27.26	5.89	11.2	156.2	16.57	38.04	4.65	16
BaTiO_3 crystal [001]	4.036	64.38	15.70	168	86	0.56	0.26	30.98	8.75	9.7	174.5	19.86	40.99	5.39	3
BaTiO_3 crystal [100]	3.990	64.38	8.93	2920	0	0	0	11.05	11.05	54.2	3
BaTiO_3 ceramic	4.036	64.38	8.85	1350	145	0.45	0.21	16.19	6.20	36.6	17.6	11.20	48.46	1.15	3
PbTiO_3 crystal (LGD)	4.152	63.28	33.30	65	78	0.56	0.76	70.85	19.87	4.0	1320.6	45.36	30.47	37.95	17
PbTiO_3 ceramic	4.152	63.28	7.31	208	46	0.40	0.76	13.90	6.01	15.1	412.2	9.95	3.95	9.93	10 Pz34
Hard PZT	4.14	67.57	14.20	1200	265	0.66	0.40	30.30	5.72	27.9	37.6	18.01	73.10	3.03	10 PIC 181
Soft PZT	4.14	67.57	19.00	2400	500	0.69	0.40	43.06	5.14	34.1	18.8	24.10	184.56	2.48	10 PIC 151
PMN-PT (111 poled)	5.81	65.5	13.30	640	190	0.69	0.42	57.99	10.55	14.5	74.1	34.27	137.52	5.91	19
PMN-PT (100 poled)	4.03	65.5	120.00	8200	2820	0.91	0.42	290.91	6.64	25.0	5.8	148.77	6145.87	3.44	19

“soft” material exhibits an effective charge 20% higher than the “hard” equivalent, its softer bond compliance (γ_1) is more than 40% larger. Arlt and Pertsev²¹ have proposed that the domain wall contributions to the primary coefficients follow the following expressions, from which an orientation factor has been omitted

$$s_{33D}^E \sim \frac{x_s^2 \gamma_D}{w}, \quad (42)$$

$$\epsilon_{33D}^X \sim \frac{P_s^2 \gamma_D}{w}, \quad (43)$$

$$d_{33D} \sim \frac{x_s P_s \gamma_D}{w}, \quad (44)$$

where x_s is the spontaneous strain, w is the domain width, and γ_D is the inverse force constant for domain wall motion. Given the similarity in form of these contributions, to the

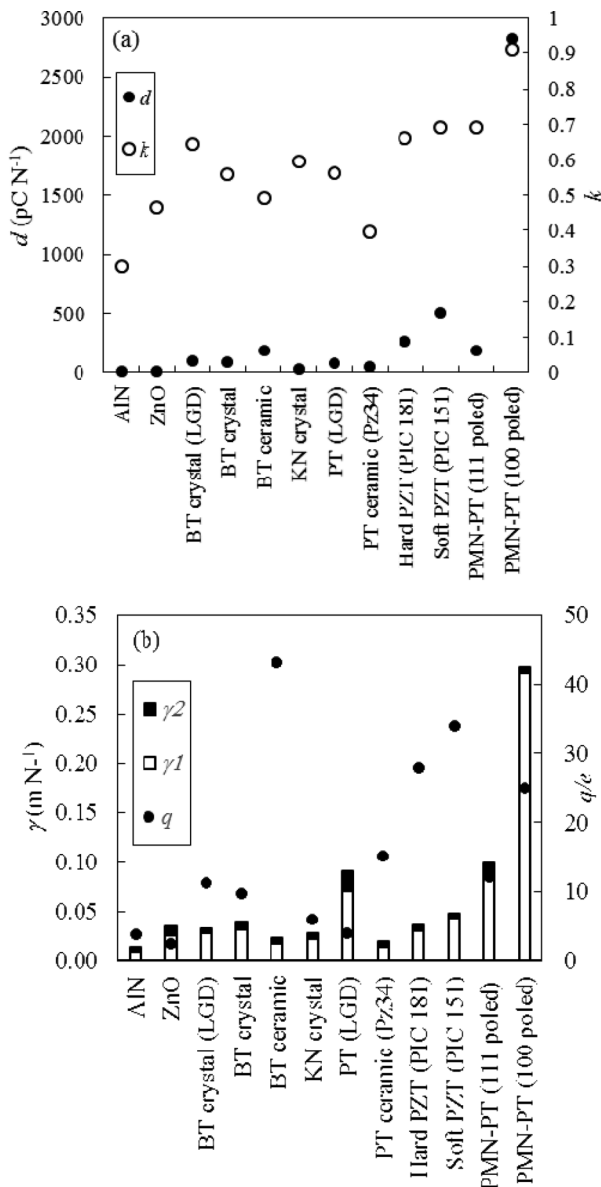


FIG. 8. (a) Experimental values of piezoelectric charge and coupling coefficients for selected materials and (b) the equivalent values of γ_1 , γ_2 , and q calculated from the model.

TABLE III. Comparison of model value of ionic displacement δ with experimental values for selected perovskites from Ref. 18.

	Experimental			Model		
	δ_B	δ_{OI}	δ_{OH}	P_s	q/e	δ
Units	pm	pm	pm	C m ⁻²		pm
BaTiO ₃	5	-9	-6	0.26	9.71	5.4
KNbO ₃	8	-13	-12	0.30	11.92	10.4
PbTiO ₃	17	-47	-47	0.76	3.96	38.0

intrinsic contributions in the 3 atom model, it is not surprising that the parameter analysis undertaken above does not distinguish between intrinsic and extrinsic contributions and assigns parameters based on the total coefficient values.

PMN-PT single crystals do not follow all the trends set by the majority of the large dataset. They have the highest values of d_{33} , ϵ_{33}^X , and k_{33} and are also amongst those with the highest s_{33}^E values. Compared to the other single crystals in Table II, they also exhibit relative high q and γ_1 values. The PMN-PT data in the large dataset are for rhombohedral crystals, with an intrinsic polar vector lying along the [111] direction. As is made clear in Table II, the largest piezoelectric coupling is observed for materials poled and then measured along the pseudo-polar [001] axis; the same materials poled and measured parallel to [111] have only moderate piezoelectric activity.¹⁹ Under [100] poling these materials exhibit, the phenomenon widely known as polarization rotation, in which under fields applied along [001], the polarization vector rotates in the (110) plane from [111] towards [001].²² Similar to the case of the dielectric anisotropy of BaTiO₃ discussed above, q is large for fields applied along [001], but in contrast to BaTiO₃, $\gamma_1 - \gamma_2$ in this direction is exceptionally large compared to the polar [111] direction. This anomalous softening is assumed to be due to the close proximity of the composition to a rhombohedral-tetragonal structural phase transition. Hence, d_{33} , ϵ_{33}^X , and k_{33} are correspondingly large for driving forces along [100].

The literature values of spontaneous polarization are also included in Table II, from which are calculated the polar displacement δ via Eq. (8). The values for BaTiO₃, KNbO₃, and PbTiO₃ are compared in Table III with the literature values of the room temperature B-site and oxygen ion shifts.²³ The calculated value of the δ parameter is smallest for BaTiO₃ and largest for PbTiO₃. The trend and values are consistent with magnitudes of the experimentally recorded shifts for the B- and O-sites across the three materials.

VI. CONCLUSIONS

Motivated by the observation that the primary electromechanical coefficients s^E , ϵ^X , and d are not mutually independent for a wide range of materials, the static, weak-field, electromechanical properties of a 3 atom, dipolar molecule have been derived in terms of the ionic charge and interatomic bond strengths. Whilst a simple, linear elastic model demonstrates the essence of the interdependence of the 3 coefficients and that the coupling coefficient k is purely a function of the bond strength asymmetry, a non-linear elastic

model is required to provide a self-consistent description for both electrostriction and piezoelectricity. Employing the model to interpret the data from a wide range of piezoelectric materials, the model demonstrates the intrinsic deception in the relationship $k = d/\sqrt{s^E \varepsilon^X}$, explaining why, counter-intuitively, k tends to correlate positively with s^E and ε^X .

The applicability of the model to real materials has been explored. Experimental electromechanical data (s^E , ε^X , d) can be parameterized in terms of an effective charge and the bond compliances (q , γ_1 , γ_2) for the linear model; in the case of ferroelectric materials for which P_s is known, the non-linear model can also yield the second order elastic coefficient η and an effective internal field E_i .

It is noted that the model does not distinguish between intrinsic and extrinsic contributions. Hence, augmentation of the primary coefficients due to domain wall motion will be expressed as changes to the effective charge and bond compliance in the same way as intrinsic phenomena.

Analysis of the parametrization for exemplar materials, emphasises that large compliance, coupled with large bond asymmetry, is necessary for maximum piezoelectric activity in single crystals. However, it also confirms that for ceramics, the dielectric anisotropy of the constituent crystal can play a key role in increasing the charge coefficient above that of the single crystal. Evaluation of the model parameters from the experimental data for a wider range of materials may prove whether the model may have some predictive, rather than a simple interpretive role in materials development.

Whilst it is difficult to experimentally test the primary outputs of the parameterization directly, the non-linear treatment for ferroelectric materials does result in values for the effective ion shifts, which when compared to the ion shifts in BaTiO₃, KNbO₃, and PbTiO₃ are of the correct magnitude and sequence. *Ab initio* density functional calculations have the potential to evaluate sub-cell bond compliances and work is currently in progress to develop a method for comparison with the 3 atom model outputs. Such a comparison would test the proposition that focusing on individual bonds may provide a rapid method of assessing new candidate piezoelectric materials through a direct calculation of the coupling coefficient from the bond strengths, thereby avoiding some of the uncertainties in calculating the polarization of new structures.

A limitation of the above analyses is the static rather than dynamic approach. Indeed, aspects of the model may be looked upon as a time-independent solution of the diatomic chain problem, which is at the heart of the successful lattice dynamics approach to ferroelectric theory. The emphasis on compliance in the static model is most probably a manifestation of the soft-mode mechanism in displacive ferroelectrics. It would be of interest therefore to examine the parallels between the two approaches more closely, particularly the practical implications of large differences in the force constants and whether there is a consistent signature for such

large differences in infra-red spectra, beyond that of a soft-mode, that may provide a rapid experimental screening technique for high activity materials.

There is also an overlap between the model and the other successful theory of ferroelectricity, the thermodynamics approach of Landau-Ginzburg-Devonshire [LGD],²⁴ which provides a description of the temperature-, field-, and stress-dependence of polarization. As permittivity and the piezoelectric charge coefficient are regarded as functions of polarization, LGD also accounts for their variation under the same variables, providing that the electrostriction coefficient is assumed to be temperature independent. However, in the basic LGD model, the elastic modulus is assumed to be independent of polarization, which is not necessarily the case in the 3 atom model. Founded on the double well potential for polarization, there is an obvious parallel between the LGD model and the non-linear elastic approach, however in the latter, the polarization comprises two independent model parameters (q and δ), both of which may be temperature dependent. Hence, to make any progress in harmonizing the current model with the LGD theory, it would be useful to carry out the parameterization of the primary coefficients for, say, BaTiO₃ as a function of temperature.

¹A. Safari and E. K. Akdogan, *Piezoelectric and Acoustic Materials for Transducer Applications* (Springer, New York, 2009).

²D. Damjanovic, *Rep. Prog. Phys.* **61**, 1267 (1998).

³H. Jaffe, W. R. Cook, and B. Jaffe, *Piezoelectric Ceramics* (Academic Press, London, 1971).

⁴J. L. Jones, M. Hoffman, J. E. Daniels, and A. J. Studer, *Appl. Phys. Lett.* **89**, 092901 (2006).

⁵V. Sundar and R. E. Newnham, *Ferroelectrics* **135**, 431 (1992).

⁶J. Grindlay and H. C. Wong, *Can. J. Phys.* **47**, 1563 (1969).

⁷Z. Suo, X. Zhao, and W. H. Greene, *J. Mech. Phys. Solids* **56**, 467 (2008).

⁸S. W. P. van Sterkenberg and Th. Kwaaitaal, *J. Phys. D: Appl. Phys.* **25**, 843 (1992).

⁹J. Curie and P. Curie, *Bull. Soc. Minéral. France* **3**, 90–93 (1880).

¹⁰See supplementary material at <http://dx.doi.org/10.1063/1.4937135> for an Excel file Piezoelectric Property Data.xls which contains all the commercial materials property data used in the paper.

¹¹R. Resta, *Rev. Mod. Phys.* **66**, 899 (1994).

¹²P. Muralt, in *Encyclopedia of Materials Science and Technology*, edited by K. H. J. Buschow, R. W. Cahn, M. C. Flemings, B. Ilschner, E. J. Kramer, S. Mahajan, and P. Veyssièrep (Elsevier, 2011), p. 8894.

¹³K. Uchino and L. E. Cross, *Jpn. J. Appl. Phys., Part 2* **19**, L171 (1980).

¹⁴T. Kamiya, *Jpn. J. Appl. Phys., Part 1* **35**, 4421 (1996).

¹⁵S. Wada, K. Muraoka, H. Kakemoto, T. Tsurumi, and H. Kumagai, *Jpn. J. Appl. Phys., Part 1* **43**, 6692 (2004).

¹⁶A. J. Bell, *J. Appl. Phys.* **89**, 3907 (2001).

¹⁷M. J. Haun, E. Furman, S. J. Jang, H. A. McKinstry, and L. E. Cross, *J. Appl. Phys.* **62**, 3331 (1987).

¹⁸M. J. Haun, E. Furman, S. J. Jang, and L. E. Cross, *Ferroelectrics* **99**, 63 (1989).

¹⁹S. Zhang and F. Li, *J. Appl. Phys.* **111**, 031301 (2012).

²⁰D. Damjanovic, *J. Am. Ceram. Soc.* **88**, 2663 (2005).

²¹G. Arlt and N. A. Pertsev, *J. Appl. Phys.* **70**, 2283 (1991).

²²B. Noheda, D. E. Cox, G. Shirane, S.-E. Park, L. E. Cross, and Z. Zhong, *Phys. Rev. Lett.* **86**, 3891 (2001).

²³M. E. Lines and A. M. Glass, *Principles and Applications of Ferroelectrics and Related Materials* (Clarendon Press, Oxford, 1977).

²⁴A. F. Devonshire, *Adv. Phys.* **3**, 85 (1954).